

Motion-corrected model-based reconstruction for 2D myocardial T1 mapping

Kirsten Miriam Kerkering¹ | Jeanette Schulz-Menger^{2,3} |
Tobias Schaeffter^{1,4} | Christoph Kolbitsch¹

¹Physikalisch-Technische Bundesanstalt (PTB), Braunschweig and Berlin, Germany

²Charité - Universitätsmedizin Berlin, corporate member of Freie Universität Berlin, Humboldt-Universität zu Berlin, and Berlin Institute of Health, DZHK (German Centre for Cardiovascular Research), partner site Berlin, Berlin, Germany

³Working Group Cardiovascular Magnetic Resonance, Experimental and Clinical Research Center, a joint cooperation between the Charité Medical Faculty and the Max-Delbrueck Center for Molecular Medicine and HELIOS Klinikum Berlin Buch, Department of Cardiology and Nephrology, Berlin, Germany

⁴Technische Universität Berlin, Department of Biomedical Engineering, Berlin, Germany

Correspondence

Kirsten Miriam Kerkering,
Physikalisch-Technische Bundesanstalt (PTB), Braunschweig and Berlin, Abbestr. 2-12, 10587 Berlin, Germany.
Email: kirsten.kerkering@ptb.de

Funding information

EMPIR, Grant/Award Number: 18HLT05 QUIERO; European Union Horizon 2020; German Research Foundation, Grant/Award Numbers: CRC1340, GRK2260-BIOQC, KO 5369/1-1

Purpose: To allow for T1 mapping of the myocardium within 2.3 s for a 2D slice utilizing cardiac motion-corrected, model-based image reconstruction.

Methods: Golden radial data acquisition is continuously carried out for 2.3 s after an inversion pulse. In a first step, dynamic images are reconstructed which show both contrast changes due to T1 recovery and anatomical changes due to the heartbeat. An image registration algorithm with a signal model for T1 recovery is applied to estimate non-rigid cardiac motion. In a second step, estimated motion fields are applied during an iterative model-based T1 reconstruction. The approach was evaluated in numerical simulations, phantom experiments and in in-vivo scans in healthy volunteers.

Results: The accuracy of cardiac motion estimation was shown in numerical simulations with an average motion field error of 0.7 ± 0.6 mm for a motion amplitude of 5.1 mm. The accuracy of T1 estimation was demonstrated in phantom experiments, with no significant difference ($p = 0.13$) in T1 estimated by the proposed approach compared to an inversion-recovery reference method. In vivo, the proposed approach yielded 1.3×1.3 mm T1 maps with no significant difference ($p = 0.77$) in T1 and SDs in comparison to a cardiac-gated approach requiring 16 s scan time (i.e., seven times longer than the proposed approach). Cardiac motion correction improved the precision of T1 maps, shown by a 40% reduced SD.

Conclusion: We have presented an approach that provides T1 maps of the myocardium in 2.3 s by utilizing both cardiac motion correction and model-based T1 reconstruction.

KEYWORDS

model-based reconstruction, motion correction, multiparametric acquisition, myocardial tissue characterization, T1 mapping

This is an open access article under the terms of the [Creative Commons Attribution](https://creativecommons.org/licenses/by/4.0/) License, which permits use, distribution and reproduction in any medium, provided the original work is properly cited.

© 2023 Physikalisch-Technische Bundesanstalt and The Authors. *Magnetic Resonance in Medicine* published by Wiley Periodicals LLC on behalf of International Society for Magnetic Resonance in Medicine.

1 | INTRODUCTION

MRI is an important imaging modality for the detection of cardiac diseases. In the past years, quantitative imaging methods have become more important because they allow more reliable therapeutic decision-making. Quantitative imaging can help to identify pathologies affecting a whole organ or structure (i.e., diffuse pathologies) because no healthy reference tissue needs to be present in the image.¹ Cardiac MRI parameter mapping, such as T1 mapping, showed promising results for the detection of a wide range of cardiomyopathies and furthermore, it allows for classification of these diseases.^{2,3}

Commonly, for T1 mapping, images at different time points after an inversion or saturation pulse are acquired and reconstructed and in a second step, a physical model is fitted to the data to calculate the quantitative T1 maps.⁴ Model-based image reconstruction has been proposed for T1 mapping, which combines both steps and utilizes the physical model as prior knowledge during image reconstruction for data acquired with high undersampling factors to ensure robust estimation of T1-times of the brain⁵ and the myocardium.⁶

A major challenge of cardiac T1 mapping is motion due to the beating of the heart. A common approach to minimize cardiac motion artifacts is to apply cardiac gating. Nevertheless, this is very inefficient because usually only 15%–20% of the total scan time is used to obtain the required data, limiting the spatial resolution of the images and the ability to visualize small lesions. This limits the clinical use of parameter mapping. Several approaches have been proposed that reduce the required amount of data for T1 mapping to achieve scan times of 4 s per slice.^{7,8} A further reduction in scan time is desirable to increase the number of slices to be obtained in a single breath-hold and hence increase the coverage of the heart while maintaining a sufficient in-plane resolution to detect small features.

To increase the scan efficiency in parameter mapping, motion-resolved T1 mapping has been proposed but it still requires scan times of 17–23 s.⁹ Cardiac motion-corrected T1 mapping on the other hand yielded a five times higher scan efficiency and two times shorter scan times compared to gated T1 mapping methods.¹⁰ Here, standard non-Cartesian image reconstruction was applied, and fitting of the image data was performed as a post-processing step. For cardiac motion estimation, cine images with constant contrast over all cardiac phases were reconstructed. The estimated motion fields were then applied prior to T1 mapping. With this increased scan efficiency, scan time could be reduced by 50% compared to standard cardiac gating yielding a 2D T1 map in 8 s. A further decrease in scan time is challenging because not enough data are available

to reconstruct cine images with a constant contrast over all cardiac phases and therefore accurate cardiac motion estimation cannot be guaranteed.

Previous studies on motion correction (MoCo) for T1 mapping have overcome the challenge of contrast changes due to T1 recovery by estimating contrast changes in addition to motion,¹¹ using image segmentation,¹² using a generic model such as principle component analysis to separate motion and contrast changes¹³ or by using the signal model of T1 recovery during image registration.^{14,15} For the latter, image registration is carried out between reconstructed images and synthetic images predicted based on, for example, a T1 map. The synthetic images show the same contrast behavior as the reconstructed images but are all in the same reference motion phase. Therefore, this synthetic image registration approach can accurately estimate motion without being impaired by contrast changes. Nevertheless, this has so far mainly been applied to aligning images acquired with cardiac triggering and not for cardiac MoCo or model-based image reconstruction (MAP). Motion and T1 estimation have also been combined in a single optimization problem.¹⁶ Nevertheless, this leads to a complex and often ill-posed problem which is difficult to solve and is so far limited to rigid motion for T1 mapping in the brain.

In this study, cardiac motion is estimated using synthetic image registration and applied during MAP in order to achieve 2D high-resolution T1 mapping in 2.3 s per slice. Motion-corrected image reconstruction¹⁷ is combined with the previously proposed MAP approach⁵ to allow for cardiac motion-corrected MAP. Accurate motion estimation was shown for native T1 mapping in a numerical simulation, T1 times were evaluated in a T1 phantom and a feasibility study was performed with a group of 10 healthy subjects by comparison of the proposed approach to model-based reconstruction without MoCo.

2 | METHODS

An overview of data acquisition, motion estimation, and MoCo is shown in Figure 1. The method consists of three main steps. In a first step, a dynamic image I_{motion} with a high temporal resolution is reconstructed to resolve cardiac motion. A preliminary diastolic T1 map ($T1_{pre-dia}$) is obtained using only images acquired within a pre-defined diastolic window to ensure all data is in the same cardiac phase. In a second step, $T1_{pre-dia}$ is used to create synthetic images ($I_{syn-dia}$) which show the same contrast behavior as I_{motion} but without cardiac motion. Non-rigid motion estimation is then carried out between the dynamic image I_{motion} and the synthetic images to estimate cardiac motion. Non-rigid MoCo can

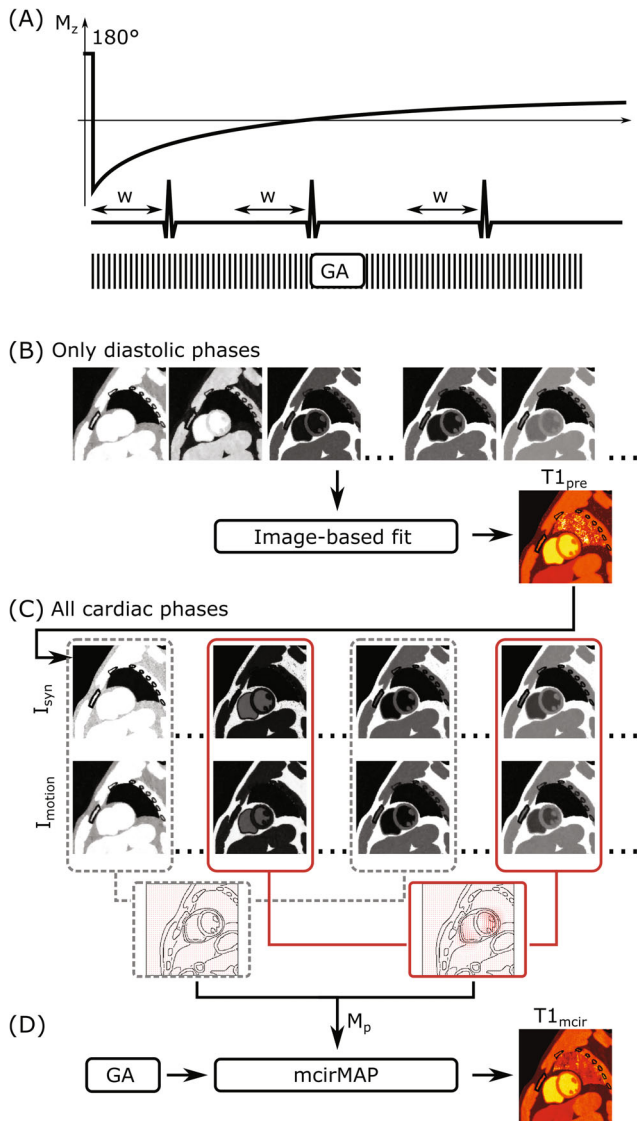


FIGURE 1 Overview of proposed cardiac motion estimation. (A) Golden angle (GA) radial data are acquired continuously for 2.3 s after an inversion pulse (180°). (B) A preliminary T1 map ($T1_{pre-dia}$) is obtained from images reconstructed from data obtained within a pre-define diastolic window (w in (A)). (C) Based on $T1_{pre-dia}$, synthetic images ($I_{syn-dia}$) are calculated which show the same contrasts as the acquired images (I_{motion}) but without cardiac motion. I_{motion} is then registered to the corresponding $I_{syn-dia}$ to estimate cardiac motion. (D) The acquired data (GA) and the obtained non-rigid motion fields (M_p) are then used in a motion-corrected MAP (mcirMAP) to obtain the final T1 maps ($T1_{mcir}$).

either be carried out after image reconstruction using a reconstruct-transform-average (RTA) approach or during image reconstruction using motion-corrected image reconstruction (mcir).¹⁷ For mcir, a motion-corrected reconstruction is carried out at each iteration of MAP rather than transforming once the images after image reconstruction.

In a third and final step of the approach, the estimated cardiac motion fields (M) are then applied in a motion-corrected MAP reconstruction (mcirMAP) to obtain the final T1 map ($T1_{mcir}$).

These steps are explained in more detail in the following. For simplicity, we will focus on the T1 map. Nevertheless, for all parameter estimations, a three-parameter model is used yielding $T1$, the equilibrium magnetisation M_0 and the apparent flip angle α .

2.1 | Data acquisition

Data were acquired continuously using an RF-spoiled gradient echo sequence with a radial trajectory. A golden angle (111.25°) was chosen between adjacent lines and global inversion pulses were applied as described in⁶ (Figure 1A). 2D slices were measured with the following scan parameter: flip angle: 5° , TE: 2.03 ms, TR: 4.93 ms, FOV: $320 \times 320 \text{ mm}^2$ with two-fold oversampling in radial direction, spatial resolution: $1.3 \times 1.3 \times 8.0 \text{ mm}^3$. The beginning of data acquisition was triggered to mid-diastole to allow estimation of M_0 and thus T1 in a diastolic window and the electrocardiogram (ECG) was recorded during the scan. Only the beginning of the scan was triggered and the rest of the data acquisition was carried out continuously without further triggering.

We compared the proposed cardiac mcirMAP to the previously proposed cardiac-gated MAP (16 s MAP) that serves as reference [6]. Therefore, data acquisition was carried out for 16 s per slice with an inversion pulse applied every 2.3 s. For the 16 s MAP, diastolic phases of the whole 16 s acquisition were used. For mcirMAP, only the first 2.3 s (i.e., data acquired after the first inversion pulse) were utilized.

2.2 | Signal model

The MR signal after the n -th RF pulse of the continuous data acquisition can be described by the transient magnetisation M_{zn} ¹⁸:

$$M_{zn} = M_{zss} + (M_s - M_{zss}) \left(\cos \alpha e^{-\frac{TR}{T1}} \right)^n \quad (1)$$

with the flip angle α , the repetition time TR and the steady-state magnetisation M_{zss} :

$$M_{zss} = M_0 \frac{1 - e^{-TR/T1}}{1 - \cos \alpha e^{-TR/T1}} \quad (2)$$

After an inversion pulse the starting magnetisation M_s is assumed to be $-M_0$. By introducing the effective T1

relaxation time $T1^*$:

$$T1^* = \frac{TR}{\frac{TR}{T1} - \ln \cos \alpha} \quad (3)$$

and Eq. (1) can be written as:

$$M_{zn} = M_{zss} - (M_0 + M_{zss}) e^{-\frac{nTR}{T1^*}} \quad (4)$$

Therefore, we can use a three-parameter model ($T1$, M_0 , α) to describe the signal behavior of the continuous data acquisition after the inversion pulse.

2.3 | Reconstruction of the dynamic image

To estimate cardiac motion, the acquired golden radial data (K) is split into different time frames, each with 16 radial lines, leading to a temporal resolution of 80 ms. A sliding window approach with a 50% overlap (8 radial lines) was used. The dynamic image I_{motion} is reconstructed using iterative image reconstruction with total variation regularization along space and time^{19,20}:

$$I_{motion} = \underset{I}{\operatorname{argmin}} \|AI - K\|_2^2 + \lambda_s \|T_s I\|_1 + \lambda_t \|T_t I\|_1 \quad (5)$$

where A is the acquisition model describing the effects of phase-array receiver coils, Fourier transformation and k-space sampling. A NUFFT-based approach was used for the non-Cartesian Fourier transformation.²¹ T_s and T_t describe the spatial and temporal total variation operator, respectively. I is a 1D image vector of length $N * N * N_{dyn}$, where N is the number of voxels along one spatial image dimension and N_{dyn} describes the number of images in I_{motion} at different time points.

I_{motion} show contrast changes due to T1 recovery and anatomical changes due to cardiac motion. A preliminary T1 map $T1_{pre-dia}$ is estimated by applying an image-based fit only to I_{motion} acquired in mid-diastole (Figure 1B). For this, an acquisition window w is defined for a mid-diastolic phase, and only images within w are utilized to estimate $T1_{pre-dia}$. Based on $T1_{pre-dia}$, a synthetic data set $I_{syn-dia}$ is created which has the same contrast changes as I_{motion} , but with all images in the same cardiac reference phase (i.e., mid-diastole) to ensure that cardiac motion estimation is not affected by the contrast changes. Both $I_{syn-dia}$ and I_{motion} show the same contrast behavior but only I_{motion} also shows cardiac motion with respect to the mid-diastolic phase.

The quality of $T1_{pre-dia}$ depends strongly on how much data is available within w and is therefore dependent on the heart rate (HR). In order to ensure robust

motion estimation even for high HR , the above steps of image selection within w , calculation of $T1_{pre-dia}$ and motion estimation are repeated three times with increasing w . The length of w is calculated based on the heart rate (HR), e.g., for 80 bpm $w = [183 \text{ ms}, 221 \text{ ms}, 259 \text{ ms}]$. For iterations 2 and 3, the motion fields of the cardiac phases M_p , determined in the previous iteration, is applied to I_{motion} for the estimation of $T1_{pre-dia}$ to ensure $T1_{pre-dia}$ is estimated in the reference motion phase without motion artifacts. Therefore, in the first iteration $T1_{pre-dia}$ is estimated from all images of I_{motion} which are within w using an image-based fit. In the following iteration, w is increased and $I_{motion} \circ M_p$ is used for the image-based fit.

The calculation of systolic (T_{sys}) and diastolic (T_{dia}) times in ms is dependent on HR and is carried out based on²²:

$$T_{sys} = 546 \text{ ms} - 2.1 \text{ HR} \text{ and } T_{dia} = 60000 \text{ ms}/HR - T_{sys}. \quad (6)$$

These times are then used to calculate the position of w such that data in mid-diastole is included.

$T1_{pre-dia}$ is a first estimate of T1 to generate $I_{syn-dia}$, but it does not have sufficient quality for diagnostic purposes, since it is estimated using only a small part of the available data and thus requiring strong regularization. The regularized reconstruction in Eq. (5) strongly reduces undersampling artifacts, but it will impair the visualization of small features. These small features will not impact cardiac motion estimation but might have high diagnostic importance. Therefore, $T1_{pre-dia}$ is not used as the final diagnostic T1 map, but in a second step mcirMAP is carried out to obtain a T1 map which is not impaired by this regularization.

2.4 | Non-rigid cardiac motion estimation

A non-rigid motion estimation approach is used to estimate cardiac motion by comparing I_{motion} to the corresponding (i.e., same contrast) $I_{syn-dia}$, because varying contrast precludes naïve cardiac binning. One challenge here is that, although the contrast in $I_{syn-dia}$ and I_{motion} is the same, there can still be images where there is poor contrast between important cardiac features (e.g., blood pool and myocardium having the same signal intensity) which would not allow for cardiac motion estimation using this intensity-based motion estimation approach. Here we are utilizing the fact that more than one cardiac cycle is covered by our acquisition. Therefore, image registration is not just carried out pairwise, but a motion field M_p for a certain cardiac phase p is estimated by registering all

image pairs $I_{syn-dia}$ and I_{motion} across multiple heartbeats, which are in cardiac phase p . Even if one image pair has poor image contrast (e.g., first image pair in Figure 1C for M_1), it is very likely that another image pair (e.g., second image pair in Figure 1C for M_1) shows sufficient contrast between blood and myocardium for accurate motion estimation. A spline-based registration algorithm²³ is used to estimate the non-rigid cardiac motion

$$M_p = \operatorname{argmin}_M \left(\sum_n S(I_{syn}^n, I_{motion}^n \circ M) + \gamma R(M) \right) \quad (7)$$

jointly across multiple heartbeats, where the index n describes all images which are in cardiac phase p . S calculates the difference between the reference images I_{syn}^n and the images I_{motion}^n transformed by M and is based on normalized mutual information. Mutual information was chosen to ensure robust motion estimation even in the case of residual contrast differences between I_{syn}^n and I_{motion}^n . The regularization R ensures smooth motion fields in the presence of undersampling artifacts in I_{motion}^n by penalizing the bending energy of the splines. We used MIRTk with a spline distance of 8 and a bending energy penalty with $\gamma = 10^{-4}$.

2.5 | Motion-corrected MAP reconstruction

After non-rigid cardiac motion estimation, the raw k-space data K and M_p are included in the mcirMAP approach to estimate the final T1 map ($T1_{mcir}$). A flowchart of mcirMAP is depicted in Figure 2.

In a first step, the radial k-space data K is separated into multiple time frames c describing the contrast changes during T1 recovery. Because the MoCo is included in the image reconstruction, the number of radial lines for each c can be defined independently of the temporal resolution of I_{motion} . In a second step, the radial lines in each c are further separated into different cardiac phases p . Because each time frame d only covers a small fraction of a cardiac cycle, there can be many combinations of (c, p) which do not have any data. This yields the k-space data $K_{(c,p)}^{acq}$ which is then interpolated to a Cartesian grid using a kernel based on.²⁴

In each iteration i , the following steps are carried out:

- Reconstruct images $I_{(c,p)}$ from $K_{(c,p)}^{acq}$ using FFT.
- Transform all cardiac phases to a reference phase and sum over cardiac phase dimensions: $I_c = \sum_p I_{(c,p)} \circ M_p$
- Carry out three-parameter fit and estimate $(T1, M_0, \alpha)_i$

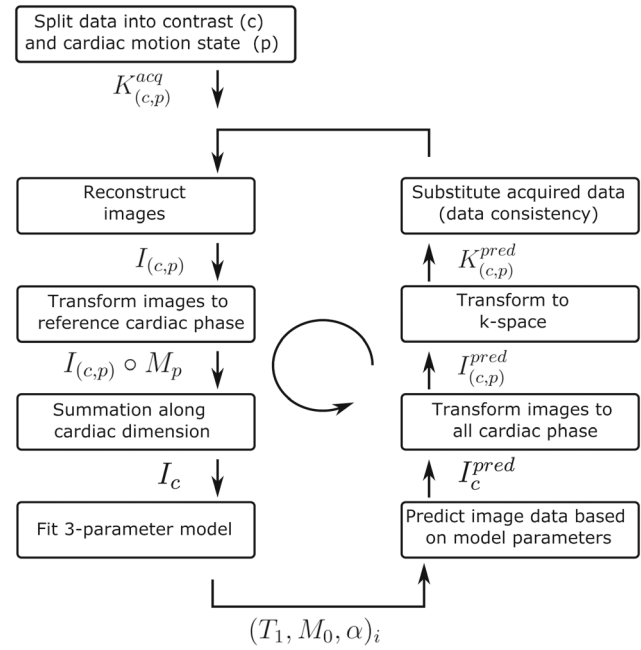


FIGURE 2 Flowchart of the proposed motion-corrected MAP approach. T1 maps are reconstructed iteratively. One iteration i consists of the reconstruction of images at different cardiac motion states and contrasts, MoCo using the motion fields M_p , T1 estimation, and prediction of image data based on the fitting results. The predicted images are transformed to k-space and the originally acquired data is substituted into the k-space for data consistency. This adapted k-space is the input for the following iteration.

- Calculate the image representation I_c^{pred} based on $(T1, M_0, \alpha)_i$
- Transform I_c^{pred} using the inverse motion fields to obtain $I_{(c,p)}^{pred}$.
- Calculate the k-space representation $K_{(c,p)}^{pred}$ of $I_{(c,p)}^{pred}$.
- Ensure data consistency by substituting all acquired k-space data in $K_{(c,p)}^{pred}$ with $K_{(c,p)}^{acq}$.

The above iterations are carried out for a fixed number of iterations until the parameter estimation has converged. In this study, the number of iterations was chosen empirically as 24 and the number of radial lines in each c was chosen to be 34. This approach is similar to the motion-corrected image reconstruction proposed by Batchelor et al. and applied to a wide range of different qualitative MRI approaches.^{17,25–27} Cardiac MoCo and T1 mapping are therefore separated and can be individually optimized. This is not the case for approaches that carry out motion estimation and correction directly on I_c .

The proposed motion estimation and correction scheme can only correct for in-plane motion. Especially during peak systole, the contraction of the heart can lead to strong through-plane motion. To ensure this does not

impair the accuracy of the T1 estimation, data acquired during 30% of the systole (calculated based on Eq. 6 and²²) were excluded in mcirMAP.

2.6 | Simulation

The numerical phantom was based on the XCAT anatomical and cardiac motion model.²⁸ An acquisition of a short-axis slice in a subject with an HR of 50, 80, and 100 bpm was simulated similarly to.²⁹ T1 times were set to 1250 ms for myocardium and other soft tissue, 1800 ms for blood and 300 ms for fat tissue. M_0 for bone was set to 0 and for lung, it was set to 1% of the M_0 of myocardium. An ECG signal recorded during an in vivo scan (HR: 80 bpm) was used to determine which radial line has been acquired in which cardiac phase. The amplitudes of the cardiac motion were chosen as provided by the cardiac motion model of XCAT. All acquisition parameters (spatial resolution, FOV, TE, TR, flip angle) were chosen identically to the in-vivo scans. Coil sensitivity maps were taken from an in-vivo scan and reoriented to fit the numerical phantom. A Gaussian smoothing filter with a width of 0.5 pixel was applied in image space to take partial volume effects into account during the forward simulation. Complex Gaussian noise with σ of 10^{-3} * maximum of the k-space was added to the simulated k-space data. As reference, a simulation without cardiac motion was also carried out and reconstructed using 16 s MAP. In addition to comparing the obtained T1 maps, the numerical simulation also allowed for the evaluation of the obtained cardiac motion fields and the impact of underestimated motion fields on the resulting T1 map. For this, the motion field was reduced to 80%, 60%, 40% and 20% of the ground-truth motion field.

2.7 | Experiments

Three different experiments were performed to test the proposed approach: a numerical phantom analysis for evaluation of motion estimation, T1 mapping in a static T1 phantom for T1 mapping accuracy, and an in vivo study to test the feasibility of the approach. For all experiments the following image reconstructions were carried out:

- 16 s MAP: Reference method using MAP reconstruction as proposed in reference⁶. Full diastolic data over the course of the 16 s scan was used. A window of 150 ms in mid-diastole was selected in each cardiac cycle to minimize motion artifacts.

- 8 s MoCo: Method using image-based MoCo and no model-based reconstruction as proposed in reference¹⁰. The first 8 s of the acquired data was used and 30% of the systole was excluded.
- 2 s MAP: MAP reconstruction of the first 2.3 s of the data acquisition. Data acquired during 30% of the systole were excluded. No cardiac MoCo was carried out.
- 2 s mcirMAP: Proposed cardiac motion-corrected MAP reconstruction of the first 2.3 s of the data acquisition. Data acquired during 30% of the systole were excluded.

In the numerical simulation, MAP reconstruction was also carried out using all the data from the 2.3 s acquisition without excluding systole (2 s MAP ungated). Data acquisition was carried out on a 3T (Verio, Siemens Healthineers, Erlangen, Germany). All image reconstruction was carried out using Python.

To evaluate T1 mapping accuracy, the approach was applied to a static T1 phantom with nine tubes with T1 times between 255 ms and 1900 ms.³⁰ The same ECG signal used for the numerical simulation was also applied here with an HR of 50 bpm and 80 bpm. As reference, T1 times were obtained by inversion-recovery spin echo (IR-SE) sequence with seven TIs between 25 and 4800 ms (TE: 12 ms, TR: 8000 ms, spatial resolution: $1.3 \times 1.3 \times 8 \text{ mm}^3$ and FOV: $130 \times 160 \text{ mm}^2$). A two-parameter fit was performed voxel-wise to estimate reference T1 times and M_0 . For accuracy estimation, T1 times of IR-SE reference and our approach were averaged over a region-of-interest manually selected in the nine tubes. Pearson's linear correlation was obtained between the two methods and differences were tested by a paired t-test.

In vivo measurements were performed in a group of 10 healthy subjects (4 females/6 males, age: $32 \pm 8 \text{ y}$). The study was approved by the institutional ethics committee and subjects gave written informed consent before the measurement. The 2D short-axis slices in the mid-ventricular myocardium were acquired. For comparison, a 3(3)3(3)5 MOLLI measurement was applied with a TR of 2.7 ms, TE of 1.12 ms, a FOV of $360 \times 307 \text{ mm}^2$, a spatial resolution of $2.1 \times 1.4 \times 8.0 \text{ mm}^3$, interpolated to $2.1 \times 1.4 \times 8.0 \text{ mm}^3$, MoCo and a flip angle of 35° in nine subjects.

In the T1 maps obtained from the numerical simulation and the in vivo acquisitions, the myocardium of the left ventricle was divided into six segments, as described in the consensus statement of the American Heart Association.³¹ Mean T1 and the SD were calculated within each segment. In the healthy myocardium, T1 times are expected to be constant within each segment. The SD of each segment can therefore be seen as a measure for the precision of the measurement. The lower the SD, the higher the precision. Mean T1 and SD were averaged

over the group of subjects for each segment. Differences between 16 s MAP, 2 s MAP, MOLLI, and 8 s MoCo compared to the proposed 2 s mcirMAP were evaluated with a Friedman test using Dunn's multiple comparison correction. All segmentations were performed using in-house software in Matlab 2016b and GraphPad Prism 8 was used for statistical analysis.

3 | RESULTS

Compared to the 16 s MAP reference method, where only 150 ms of each cardiac cycle were used to minimize cardiac motion artifacts, scan efficiency was increased from

$16.8\% \pm 2.9\%$ for the 16 s MAP approach to $86.5\% \pm 3.3\%$ with the proposed cardiac MoCo. With this increased efficiency, T1 mapping within 2.3 s was possible, reducing the overall scan time by a factor of 7. Figure 3 shows the results of the numerical simulations for 80 bpm. The estimated motion vector fields (M) were well aligned to the ground truth motion vector fields (M_{ref}) obtained from the XCAT simulation (Figure 3A). A perfect alignment was not to be expected because M was calculated relative to an image reconstructed within a mid-diastolic window w , whereas M_{ref} was relative to end-diastole. Still, the average difference between M_{ref} and M in the myocardium was only 0.7 ± 0.6 mm for a motion amplitude of 5.1 mm in M_{ref} . The estimated T1 maps with and without MoCo

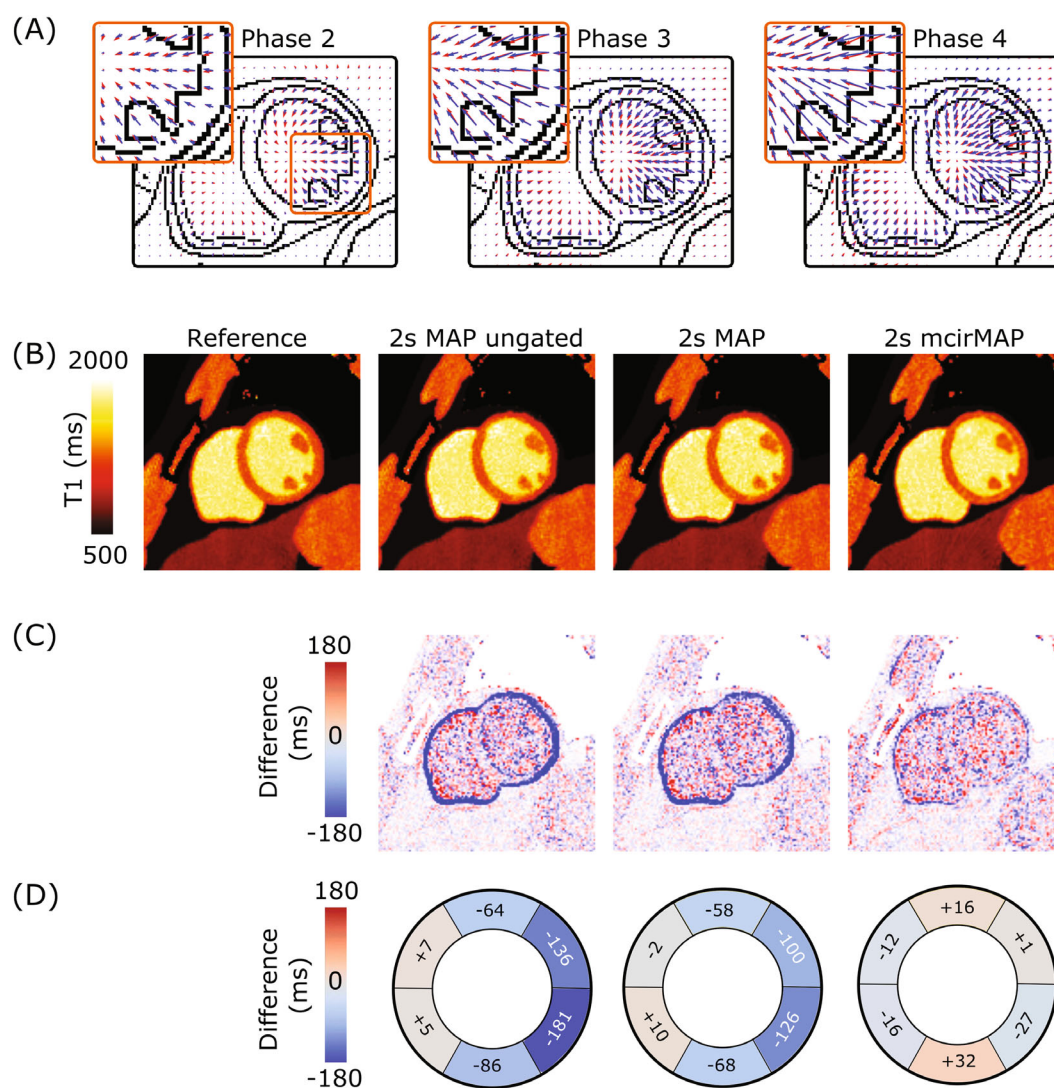


FIGURE 3 Results of the numerical simulations. (A) Estimated (red) and ground truth (blue) motion fields for selected cardiac phases with large motion amplitude. (B) Estimated T1 maps estimated without motion (Reference), using all data (2 s MAP ungated), without 30% of systolic time frames (2 s MAP) and using the proposed motion-corrected MAP approach, without 30% of systolic time frames (2 s mcirMAP). (C) Pixel-wise difference to the reconstructed motion-free reference image. (D) Bull's eye plot showing differences from the reconstructed reference image.

and their difference from the reference T1 map are shown in Figure 3B, C. The difference as a bull's eye plot is also given in Figure 3D. Cardiac motion led to errors in T1 quantification of more than 150 ms, especially in segments with large cardiac motion amplitudes and segments where the myocardium borders epicardial fat and lung tissue. Motion artifacts were strongly reduced with the proposed mcirMAP approach. An overview of the results for an HR of 50, 80, and 100 bpm can be found in Figure S1. The reconstruction time for 2 s mcirMAP was 110 min, compared to 5 min for 2 s MAP, 4 min for 16 s MAP, and 20 min for 8 s MoCo. Simulation results using different numbers of iterations can be found in Figure S2. Underestimation of the motion fields led to differences in T1 estimation, which can be found in Figure S3.

In the T1 phantom, high correlation was found between the 2.3 s T1 mapping approach and reference IR-SE data ($R > 0.99$, Figure 4). For the vial representing medium native myocardium, IR-SE led to a T1 time of $1220 \text{ ms} \pm 14 \text{ ms}$ compared to $1215 \text{ ms} \pm 65 \text{ ms}$ and $1213 \text{ ms} \pm 34 \text{ ms}$ for 16 s MAP and 2 s MAP, respectively. For the tube representing normal native blood, IR-SE led to a T1 time of $1900 \text{ ms} \pm 38 \text{ ms}$, compared to $1978 \text{ ms} \pm 81 \text{ ms}$ and $2000 \text{ ms} \pm 73 \text{ ms}$ for 16 s MAP and 2 s

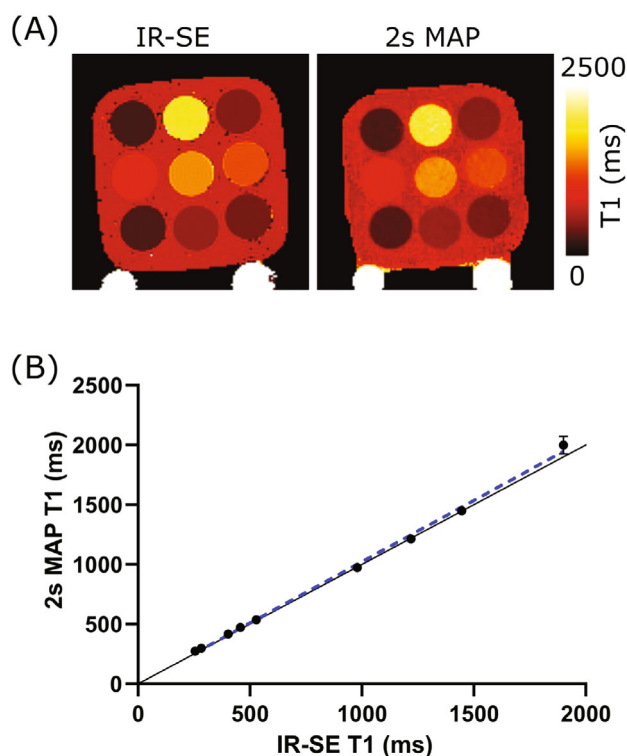


FIGURE 4 Phantom evaluation (80 bpm). (A) For all T1 times between 255 ms and 1900 ms, T1 mapping within 2.3 s (2 s MAP) showed good agreement with the IR-SE reference measurement. (B) No statistically significant differences were found between reference IR-SE T1 mapping and 2 s MAP.

MAP (all values obtained for an HR of 80 bpm). T1 times of all vials and for HRs of 50 bpm and 80 bpm can be found in Table S1. No significant differences were found between the IR-SE reference and 2 s MAP (difference over all tubes: $17.98 \text{ ms} \pm 31.93 \text{ ms}$, $p = 0.13$), and a slope of 1.026, with its confidence interval [0.98 1.069] was obtained by linear regression.

For the in vivo measurements, the HR was varying between 44 and 82 bpm ($62 \pm 10 \text{ bpm}$). Figure 5 compares I_{motion} to $I_{syn-dia}$ for one volunteer with an HR of 65 bpm. $T1_{pred}$ in the first and third (last) iteration are also shown. $I_{syn-dia}$ shows similar contrast behavior as I_{motion} but all images are in the same motion state.

Examples of cardiac MoCo are shown in Figure 6 for two subjects. The contrast changes due to T1 recovery after the inversion pulse can be seen in the images and also in the temporal-spatial time plot. In addition, contraction and relaxation of the heart during – in this case two – cardiac cycles can also be seen. After transformation of these images with the estimated motion fields, the contrast changes were still present, but the individual images were all in the same cardiac motion state. The transformation of I_{motion} was here only carried out to show the effect of the estimated motion fields but T1 was not estimated from these images but using mcirMAP, by integrating the motion fields M into the image reconstruction.

Motion led to wrong T1 estimation in the myocardium (Figure 7, subject 1) in T1 maps obtained with 2 s MAP. Furthermore, small features with large motion amplitudes, such as the papillary muscles, showed more blurring (Figure 7, subjects 2 and 3) compared to the 16 s MAP reference measurement. The proposed 2 s mcirMAP approach corrected for these motion artifacts and ensured myocardial T1 estimation without significant differences to 16 s MAP method and small structures were as visible as in MOLLI and 8 s MoCo T1 maps. A decrease in scan time using the 8 s MoCo method yielded differences in contrast over the cardiac phases and therefore accurate cardiac motion estimation cannot be guaranteed, which can be seen in Figure S4. In Figure 8, T1 times and SDs over all subjects within the six segments are shown. In the group of healthy subjects, no statistically significant differences were found between 16 s MAP T1 times and T1 times obtained with the 2 s mcirMAP approach (mean T1 time over all segments and volunteers, 16 s; MAP, $1251 \text{ ms} \pm 62 \text{ ms}$; mcirMAP T1, $1250 \text{ ms} \pm 50 \text{ ms}$; $p = 0.77$). The SD for 2 s mcirMAP (median and interquartile range: 66 (24) ms) was lower compared to 16 s MAP (109 (49) ms, $p < 0.0001$). Compared to MOLLI, myocardial T1 values and SDs in myocardium and blood were higher. Without model-based reconstruction (8 s MoCo), T1 times in myocardium and blood were shorter, but the precision did

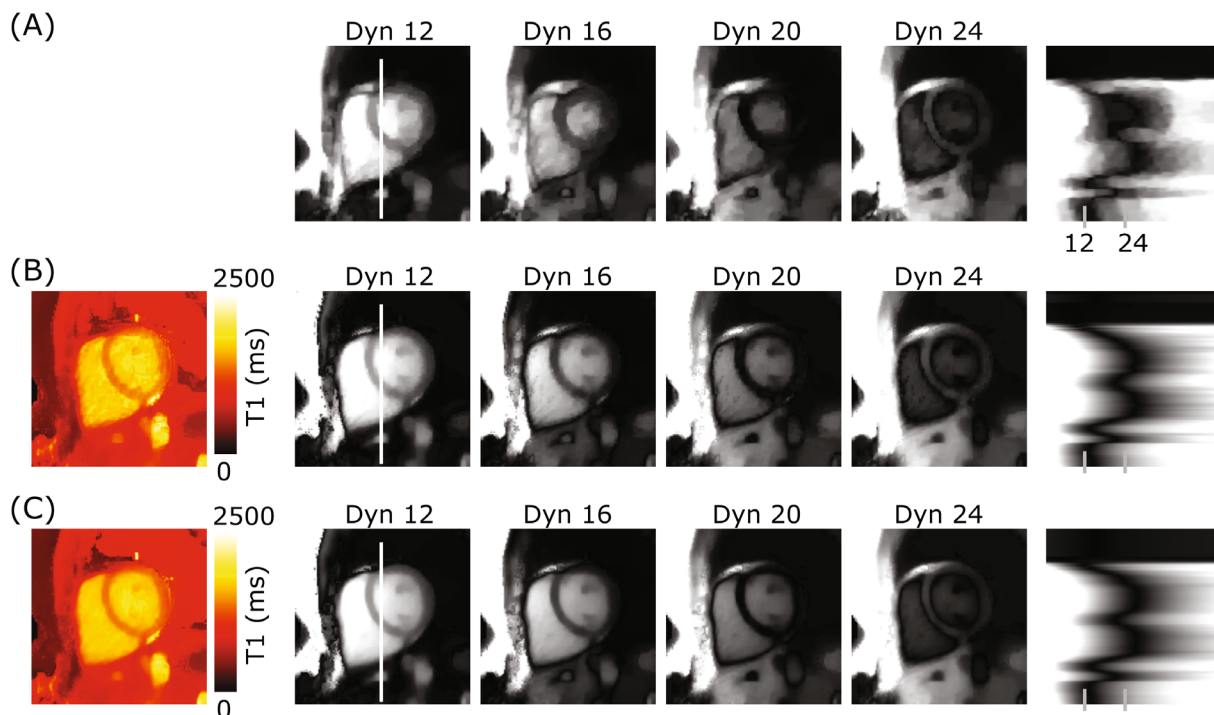


FIGURE 5 (A) Dynamic image I_{motion} reconstructed from one volunteer with an HR of 65 bpm. Four different images (Dyn 12, 16, 20, and 24) are shown and a spatial-temporal plot along the white line indicated in image 12. $T1_{pred}$ and $I_{syn-dia}$ are shown for iteration 1 (B) and iteration 3 (C). The brightness of the images was adapted for each time point of I_{motion} separately to improve visibility. The final T1 map of this volunteer is shown in Figure 7, subject 2.

not differ from 2 s mcirMAP. Results are summarized in Table 1.

4 | DISCUSSION

In this study, we demonstrated that 2D T1 mapping of the myocardium is possible in 2.3 s by combining MAP and cardiac MoCo. Phantom measurements did not show any significant differences in T1 estimation compared to an IR-SE reference method. Numerical simulations confirmed the improvement achieved with cardiac MoCo. In vivo scans showed high agreement between the proposed 2 s mcirMAP and a 16 s reference scan. Small structures were as

Motion estimation was carried out relative to a diastolic reference phase. This reference phase was initially calculated from data within a window w with a similar size to the gating window used for 16 s reference reconstruction. Although the window w was increased during the iterative motion estimation, the final cardiac motion fields describe the transformation to the initial reference phase very well because the motion estimation from the previous iteration is already used for image-based MoCo. In the case of an HR of 80 bpm, when w is increased from 183 ms to 221 ms, then, the cardiac motion estimated for

$w = 183$ ms, is already used to correct the newly added data. This can also be seen in Figure 3, where the 2 s mcirMAP shows very little difference to a motion-free late diastolic T1 map, although the final window size w was as large as 260 ms.

Motion during peak systolic contraction is challenging to estimate because of two reasons. On the one hand, motion velocities are very high and therefore motion is difficult to accurately resolve in the dynamic image I_{motion} . In addition, through-plane motion occurs during systolic contraction which cannot be corrected for in 2D imaging. To minimize any errors due to these two effects, 30% of systole was excluded from image reconstruction for 2 s mcirMAP. For an HR of 80 bpm, this would correspond to excluding data within a window of 113 ms placed around peak systole. The value of 30% was chosen based on previous studies but could be further optimized. So far, the systolic phases were calculated based on Eq. (6). Nevertheless, peak systole could also be detected directly from the obtained motion fields.

The removal of data acquired during peak-systole, identified for each heartbeat, is also the main reason for triggering the beginning of the sequence to mid-diastole. The signal right after the inversion pulse is important to encode the equilibrium (M_0) magnetisation. If the beginning were to occur during peak-systole, this data

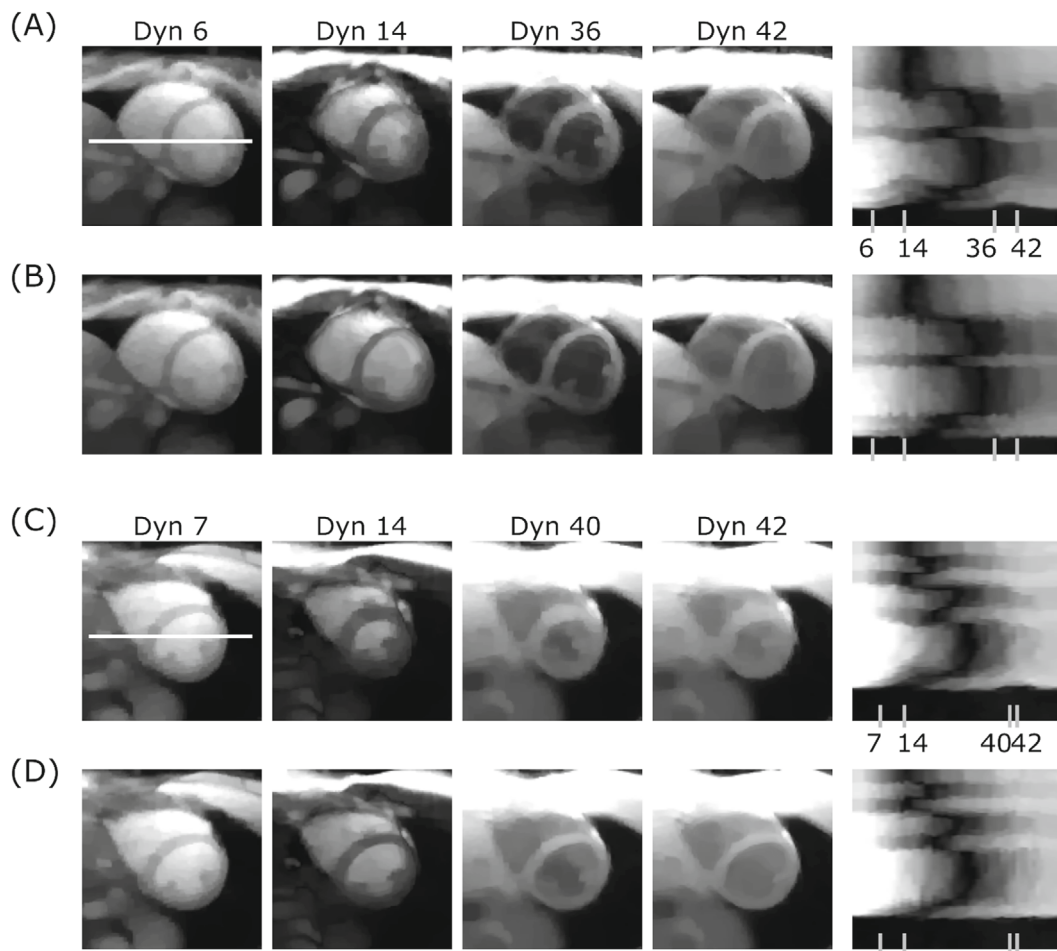


FIGURE 6 (A, B) Dynamic image I_{motion} reconstructed from two volunteers according to Eq. (5) showing contrast changes due to an inversion pulse and cardiac motion. Four different images (Dyn 6, 14, 36, and 42 and Dyn 7, 14, 40, and 42, respectively) are shown and a spatial–temporal plot along the white line indicated in images Dyn 6 and 7, respectively. (B, D) Individual images after transformation to the reference motion state with the estimated motion fields. The brightness of the images was adapted for each time point of I_{motion} separately to improve visibility.

would be discarded leading to poor estimation of M_0 and also T1.

Long T1 times (>1.5s) can be properly estimated from the 2.3s data, without significant differences to the 16s MAP approach or MOLLI, possibly due to the iterative T1 estimation within the model-based reconstruction. Image-based approaches, such as 8s MoCo, however, lead to shorter T1 times in blood which can be seen in Table 1. The precision of the different methods was evaluated in Figure 8, based on the SD of the different myocardial segments. The precision of 2s mcirMAP T1 mapping is lower compared to MOLLI. This could be caused by differences in acquisition parameters and the post-processing steps of the qualitative images before T1 mapping, such as interpolation or MoCo. Further test–retest experiments are required to confirm these results. So far, we did not use any regularization in our mcirMAP approach. Nevertheless, regularization of the estimated parameter

(T_1 , M_0 , α) could lead to further improvements, especially in precision. In our approach, for example, TV-based denoising could be applied to $(T_1, M_0, \alpha)_i$ before calculating I_c^{pred} similar to.³²

Figure 7 shows a small degree of blurring of 2s mcirMAP. This is probably caused by insufficient motion estimation. An increasing error in the motion fields is leading to an increasing error in the final T1 map, as shown in Figure S3. Therefore, accurate motion estimation plays a crucial role. In this study, we carried out motion estimation and T1 mapping separately to make full use of the flexibility of continuous radial data acquisition. High temporal resolution (80ms) combined with regularized image reconstruction was used for motion estimation to ensure cardiac motion is accurately resolved. High spatial regularization could lead to smoothing of small details, but this impairs estimation of motion fields to only a small extent because motion fields are smooth

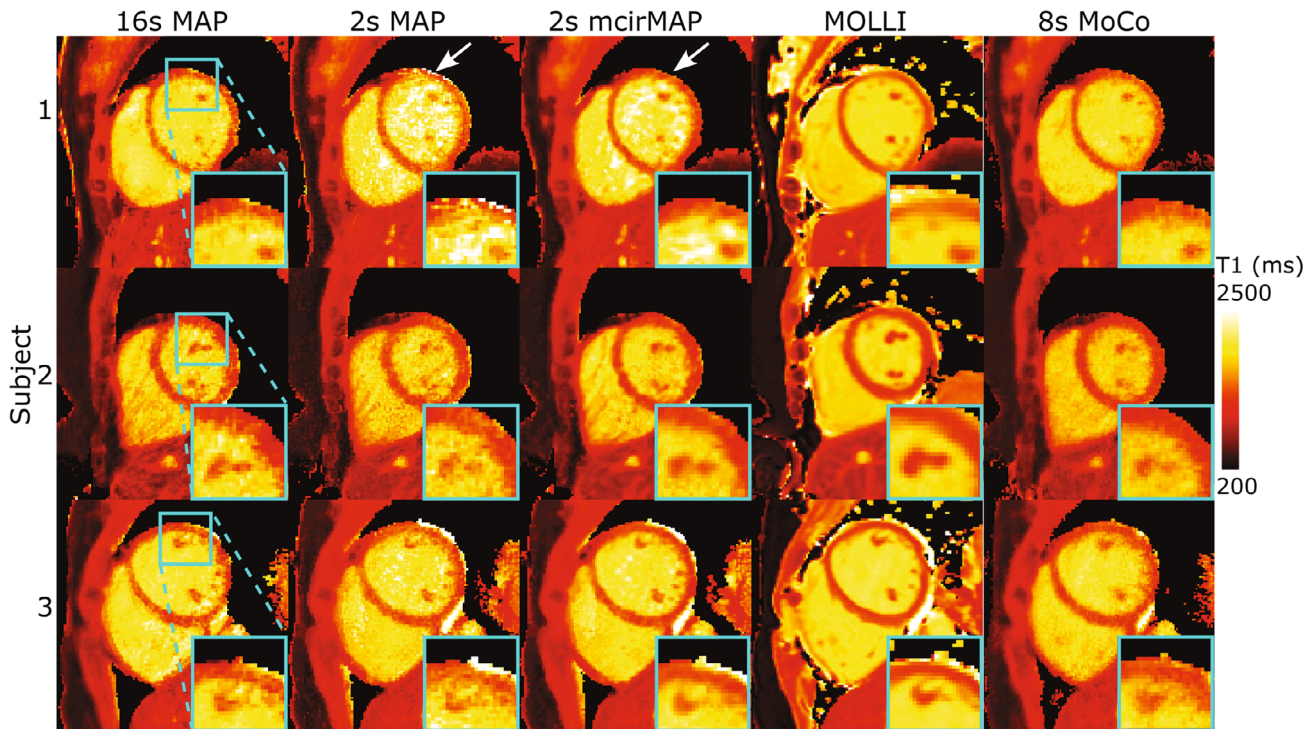


FIGURE 7 In vivo T1 maps of three healthy subjects. Compared to 16 s MAP (first column), 2 s MAP resulted in motion artifacts (second column). This can be seen by changes of T1 times in part of the myocardium (subject 1) or less well depiction of small and fast-moving tissue, such as the papillary muscle (subjects 2 and 3). By integration of cardiac MoCo (2 s mcirMAP), these inaccuracies were not present anymore (middle column) and small structures were as visible as in MOLLI and 8 s MoCo T1 maps (fourth and fifth column).

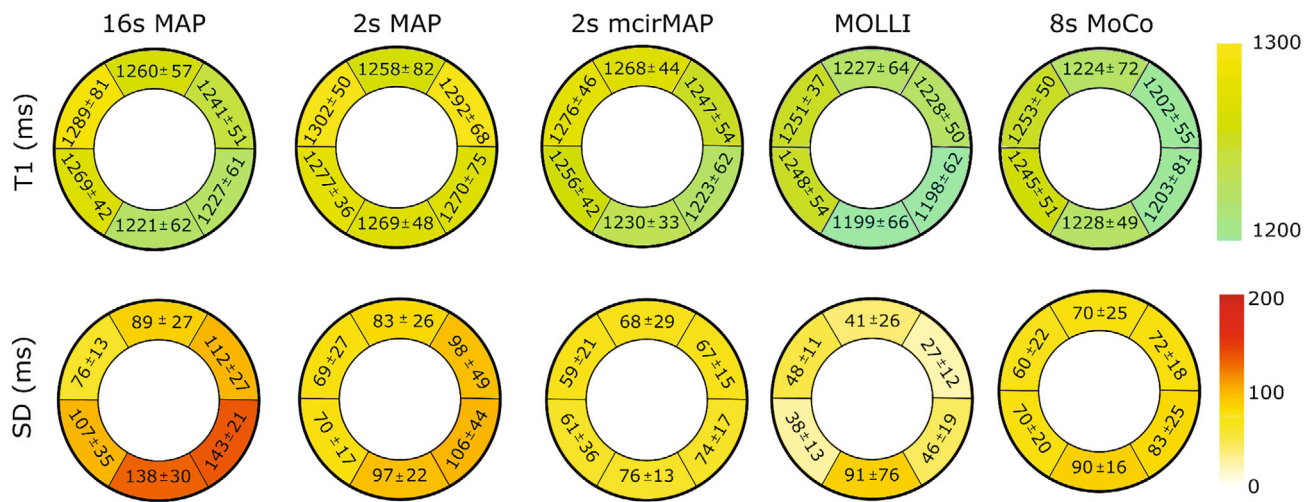


FIGURE 8 Bull's eye plots of mean T1 times and SDs obtained by the different approaches. For each segment, T1 times (first row) and SDs (second row) were averaged over the healthy subjects and represented as mean value \pm SD over the subjects. The SDs given in the second row serve as a measure of the precision of the approaches.

as well. The temporal regularization in Eq. (5) could lead to a temporal blurring and hence underestimation of cardiac motion. Nevertheless, in the numerical simulation, this was not an issue and high agreement between ground truth and estimated motion fields was achieved. In addition to the cardiac motion, the image content also changed

due to T1 recovery. These changes were much smoother than the cardiac motion and did not impair the temporal regularization. For MAP, reconstruction temporal resolution was reduced to 168 ms (i.e., using 34 radial lines for each time frame) because only T1 recovery needs to be resolved which changes much more slowly compared to

TABLE 1 Mean T1 times and SD averaged over all healthy subjects and all segments for myocardium and blood

	16 s MAP	2 s MAP	2 s mcirMAP	MOLLI	8 s MoCo
Myocardium (T1 mean \pm SD)	1251 \pm 62	1278 \pm 61***	1250 \pm 50	1225 \pm 58**	1226 \pm 61**
Myocardium (SD median (IQR))	109 (49)***	79 (41)**	66 (24)	37 (30)**	72 (29)
Blood (T1 mean \pm SD)	1843 \pm 85	1847 \pm 131	1836 \pm 117	1832 \pm 85	1777 \pm 95*
Blood (SD median (IQR))	73 (24)	105 (35)	81 (31)	27 (9)***	49 (21)

Note: Statistically significant difference of 16 s MAP, 2 s MAP, MOLLI, and 8 s MoCo compared to the proposed 2 s mcirMAP was evaluated with a Friedman test using Dunn's multiple comparison correction.

* $p < 0.05$. ** $p < 0.01$. *** $p < 0.001$. All values in ms.

cardiac motion. The lower temporal resolution allowed for T1 mapping without the need for any further regularization. An even smaller number of radial lines for each time frame could reduce any temporal blurring further but would lead to longer reconstruction times. The number of iterations was fixed to 24 iterations to ensure robust T1 fitting. For a low number of iterations (six), images appeared blurry, and a higher number of iterations lead to an increase in noise, which can be seen in Figure S2. However, noise amplification was not high, even for 192 iterations.

Cardiac MoCo has previously been combined with MAP,³³ but for late gadolinium enhancement imaging rather than T1 mapping. In this study, cardiac motion was estimated from a standard cine reconstruction using data acquired at least 3.5 s after an inversion pulse showing little contrast changes and therefore standard motion estimation could be applied.

The performance of the image registration depends on the accuracy of the initial T1 map $T1_{pre}$ used to calculate the synthetic image data. Any inaccuracies in $T1_{pre}$ will lead to contrast differences between the synthetic and dynamic image data, which might impair cardiac motion estimation. Therefore, we used normalized mutual information as an image similarity metric in Eq. (7) to ensure robust motion estimation even if there are residual contrast differences. This study did not include any subjects with irregular cardiac motion such as arrhythmia or abnormal contraction in certain myocardial segments. This could make accurate motion estimation more challenging and further optimization of the image registration might be required. For severe cases, additional arrhythmia detection and rejection would need to be done, leading to an increase in scan time. For very high HRs (i.e., 100 bpm), errors could occur, which can be seen in Figure S1. However, in our in-vivo measurements, T1 maps were obtained

with a broad range of HRs (44–82 bpm) and simulation do not show differences between 50 and 80 bpm.

The signal model described in Eq. (4) assumes that the inversion efficiency is 100% which is usually not the case.³⁴ This could lead to errors in T1 quantification.³⁵ Further improvement in T1 accuracy could be achieved by using more advanced pulses or consideration of the inversion efficiency during T1 estimation. Furthermore, changes in myocardial blood volume during the cardiac cycle, through-plane motion of the heart and the flowing blood could lead to errors in apparent T1. This can partly be compensated with a lower estimate of the apparent flip angle. In vivo T1 times were in a reasonable range, although myocardial T1 times were longer compared to MOLLI, but this is also the case in other studies^{35–38}.

MR multitasking has been proposed to overcome the challenge of cardiac motion gating for T1 mapping by utilizing the cardiac motion dimension for regularization during image reconstruction and it allows for free-breathing cardiac T1 mapping.^{39,40} Low rank reconstruction along the cardiac motion dimension was also integrated in MR fingerprinting, but scan times are in the order of 10–18 s with lower spatial resolution.^{38,41} Model-based reconstruction was also combined with respiratory motion, but scan times were 2 min and extra recovery periods were implemented in the sequence, not fully utilizing the entire scan time.⁴²

Each slice was obtained in a single breathhold, to be able to obtain enough data for the 16 s reference method. Nevertheless, with the proposed approach multiple slices could be obtained in a single breathhold. For this, the non-selective inversion pulse used would have to be replaced with a slice-selective inversion pulse to ensure high signal intensities and accurate parameter estimation for all slices. In addition, we did not correct for any residual respiratory motion. All volunteers could hold their

breath reliably. Nevertheless, for patient studies, respiratory motion estimation could be carried out similarly to the proposed cardiac motion estimation using a dynamic image with a much larger temporal footprint.^{27,43} After respiratory motion estimation, these motion fields could be integrated into the motion-corrected image reconstruction of Eq. (5). Finally cardiac motion could be estimated and then both motion types could be combined for mcirMAP.

5 | CONCLUSION

Myocardial T1 mapping in a short 2.3 s breath hold was achieved by integration of cardiac MoCo into iterative MAP. Compared to MAP without MoCo, here only 14% of the overall scan time was needed by increasing the scan efficiency from $16.8\% \pm 2.9\%$ to $86.5\% \pm 3.3\%$ to obtain native T1 maps, without loss in T1 estimation accuracy using cardiac MoCo. Furthermore, an increase in precision was shown by a 40% reduced SD.

ACKNOWLEDGMENTS

The authors gratefully acknowledge the co-funding from the German Research Foundation (GRK2260-BIOQIC, KO 5369/1-1, CRC1340 Matrix in Vision). This work was also supported by EMPIR project 18HLT05 QUIERO and received funding from the EMPIR programme co-financed by the Participating States and from the European Union's Horizon 2020 research and innovation programme. Open Access funding enabled and organized by Projekt DEAL.

ORCID

Kirsten Miriam Kerkering  <https://orcid.org/0000-0002-8165-5943>

Jeanette Schulz-Menger  <https://orcid.org/0000-0003-3100-1092>

Tobias Schaeffter  <https://orcid.org/0000-0003-1310-2631>

Christoph Kolbitsch  <https://orcid.org/0000-0002-4355-8368>

REFERENCES

- Goebel J, Seifert I, Nensa F, et al. Can native T1 mapping differentiate between healthy and diffuse diseased myocardium in clinical routine cardiac MR imaging? *PLoS One*. 2016;11:e0155591. doi:10.1371/journal.pone.0155591
- Haaf P, Garg P, Messroghli DR, Broadbent DA, Greenwood JP, Plein S. Cardiac T1 mapping and extracellular volume (ECV) in clinical practice: a comprehensive review. *J Cardiovasc Magn Reson*. 2017;18:89. doi:10.1186/s12968-016-0308-4
- Radenkovic D, Weingärtner S, Ricketts L, Moon JC, Captur G. T1 mapping in cardiac MRI. *Heart Fail Rev*. 2017;22:415-430. doi:10.1007/s10741-017-9627-2
- Taylor AJ, Salerno M, Dharmakumar R, Jerosch-Herold M. T1 Mapping. *JACC Cardiovasc Imaging*. 2016;9:67-81. doi:10.1016/j.jcmg.2015.11.005
- Tran-Gia J, Stäb D, Wech T, Hahn D, Köstler H. Model-based acceleration of parameter mapping (MAP) for saturation prepared radially acquired data. *Magn Reson Med*. 2013;70:1524-1534. doi:10.1002/mrm.24600
- Becker KM, Schulz-Menger J, Schaeffter T, Kolbitsch C. Simultaneous high-resolution cardiac T1 mapping and cine imaging using model-based iterative image reconstruction. *Magn Reson Med*. 2019;81:1080-1091. doi:10.1002/mrm.27474
- Piechnik SK, Ferreira VM, Dall'Armellina E, et al. Shortened modified look-locker inversion recovery (ShMOLLI) for clinical myocardial T1-mapping at 1.5 and 3 T within a 9 heartbeat breathhold. *J Cardiovasc Magn Reson*. 2010;12:69. doi:10.1186/1532-429X-12-69
- Wang X, Kohler F, Unterberg-Buchwald C, Lotz J, Frahm J, Uecker M. Model-based myocardial T1 mapping with sparsity constraints using single-shot inversion-recovery radial FLASH cardiovascular magnetic resonance. *J Cardiovasc Magn Reson*. 2019;21:60. doi:10.1186/s12968-019-0570-3
- Weingärtner S, Shenoy C, Rieger B, Schad LR, Schulz-Menger J, Akçakaya M. Temporally resolved parametric assessment of Z-magnetization recovery (TOPAZ): dynamic myocardial T1 mapping using a cine steady-state look-locker approach. *Magn Reson Med*. 2018;79:2087-2100. doi:10.1002/mrm.26887
- Becker KM, Blaszczyk E, Funk S, et al. Fast myocardial T1 mapping using cardiac motion correction. *Magn Reson Med*. 2020;83:438-451. doi:10.1002/mrm.27935
- Roujol S, Foppa M, Weingärtner S, Manning WJ, Nezafat R. Adaptive registration of varying contrast-weighted images for improved tissue characterization (ARCTIC): application to T1 mapping. *Magn Reson Med*. 2015;73:1469-1482. doi:10.1002/mrm.25270
- El-Rewaify H, Nezafat M, Jang J, Nakamori S, Fahmy AS, Nezafat R. Nonrigid active shape model-based registration framework for motion correction of cardiac T1 mapping. *Magn Reson Med*. 2018;80:780-791. doi:10.1002/mrm.27068
- Huizinga W, Poot DHJ, Guyader JM, et al. PCA-based group-wise image registration for quantitative MRI. *Med Image Anal*. 2016;29:65-78. doi:10.1016/j.media.2015.12.004
- Xue H, Shah S, Greiser A, et al. Motion correction for myocardial T1 mapping using image registration with synthetic image estimation. *Magn Reson Med*. 2012;67:1644-1655. doi:10.1002/mrm.23153
- Tilborghs S, Dresselaers T, Claus P, et al. Robust motion correction for cardiac T1 and ECV mapping using a T1 relaxation model approach. *Med Image Anal*. 2019;52:212-227. doi:10.1016/j.media.2018.12.004
- Ramos-Llorden G, den Dekker AJ, Van Steenkiste G, Van Audekerke J, Verhoye M, Sijbers J. Simultaneous motion correction and T1 estimation in quantitative T1 mapping: an ML restoration approach. *2015 IEEE International Conference on Image Processing (ICIP)*. IEEE; 2015:3160-3164. doi:10.1109/ICIP.2015.7351386
- Batchelor PG, Atkinson D, Irrarrazaval P, Hill DLG, Hajnal J, Larkman D. Matrix description of general motion correction applied to multishot images. *Magn Reson Med*. 2005;54:1273-1280. doi:10.1002/mrm.20656

18. Deichmann R, Haase A. Quantification of T₁ values by SNAPSHOT-FLASH NMR imaging. *J Magn Reson.* 1992;612:608-612. doi:10.1016/0022-2364(92)90347-A
19. Block KT, Uecker M, Frahm J. Suppression of MRI truncation artifacts using total variation constrained data extrapolation. *Int J Biomed Imaging.* 2008;2008:184123. doi:10.1155/2008/184123
20. Cruz G, Atkinson D, Buerger C, Schaeffter T, Prieto C. Accelerated motion corrected three-dimensional abdominal MRI using total variation regularized SENSE reconstruction. *Magn Reson Med.* 2016;75:1484-1498. doi:10.1002/mrm.25708
21. Lin JM. Python non-uniform fast fourier transform (PyNUFFT): an accelerated non-cartesian MRI package on a heterogeneous platform (CPU/GPU). *J Imaging.* 2018;4:51. doi:10.3390/jimaging4030051
22. Lewis RP, Rittogers SE, Froester WF, Boudoulas H. A critical review of the systolic time intervals. *Circulation.* 1977;56:146-158. doi:10.1161/01.CIR.56.2.146
23. Rueckert D, Sonoda LI, Hayes C, Hill DLG, Leach MO, Hawkes DJ. Nonrigid registration using free-form deformations: application to breast MR images. *IEEE Trans Med Imaging.* 1999;18:712-721. doi:10.1109/42.796284
24. Seiberlich N, Breuer FA, Blaimer M, Barkauskas K, Jakob PM, Griswold MA. Non-cartesian data reconstruction using GRAPPA operator gridding (GROG). *Magn Reson Imaging.* 2007;58:1257-1265. doi:10.1002/mrm.21435
25. Schmidt JFM, Buehrer M, Boesiger P, Kozerke S. Nonrigid retrospective respiratory motion correction in whole-heart coronary MRA. *Magn Reson Med.* 2011;66:1541-1549. doi:10.1002/mrm.22939
26. Prieto C, Doneva M, Usman M, et al. Highly efficient respiratory motion compensated free-breathing coronary mra using golden-step cartesian acquisition. *J Magn Reson Imaging.* 2014;746:738-746. doi:10.1002/jmri.24602
27. Kolbitsch C, Ahlman MA, Davies-Venn C, et al. Cardiac and respiratory motion correction for simultaneous cardiac PET/MR. *J Nucl Med.* 2017;58:846-852. doi:10.2967/jnumed.115.171728
28. Segars WP, Sturgeon G, Mendonca S, Grimes J, Tsui BMW. 4D XCAT phantom for multimodality imaging research. *Med Phys.* 2010;37:4902-4915. doi:10.1118/1.3480985
29. Wissmann L, Santelli C, Segars WP, Kozerke S. MRXCAT: realistic numerical phantoms for cardiovascular magnetic resonance. *J Cardiovasc Magn Reson.* 2014;16:1-11. doi:10.1186/s12968-014-0063-3
30. Captur G, Gatehouse P, Keenan KE, et al. A medical device-grade T₁ and ECV phantom for global T₁ mapping quality assurance – the T₁ mapping and ECV standardization in cardiovascular magnetic resonance (TIMES) program. *J Cardiovasc Magn Reson.* 2016;18:1-20. doi:10.1186/s12968-016-0280-z
31. Cerqueira MD. Standardized myocardial segmentation and nomenclature for tomographic imaging of the heart: a statement for healthcare professionals from the cardiac imaging Committee of the Council on clinical cardiology of the American Heart Association. *Circulation.* 2002;105:539-542. doi:10.1161/hc0402.102975
32. Hamilton JI, Jiang Y, Chen Y, et al. MR fingerprinting for rapid quantification of myocardial T₁, T₂, and proton spin density. *Magn Reson Med.* 2017;77:1446-1458. doi:10.1002/mrm.26668
33. Wech T, Tran-Gia J, Rützel F, Klink T, Bley TA, Köstler H. Single-shot late Gd enhancement imaging of myocardial infarction with retrospectively adjustable contrast and heart-phase. *Magn Reson Imaging.* 2018;47:48-53. doi:10.1016/j.jmri.2017.10.008
34. Kellman P, Herzka DA, Hansen MS. Adiabatic inversion pulses for myocardial T₁ mapping. *Magn Reson Med.* 2014;71:1428-1434. doi:10.1002/mrm.24793
35. Kellman P, Hansen MS. T₁-mapping in the heart: accuracy and precision. *J Cardiovasc Magn Reson.* 2014;16:1-20. doi:10.1186/1532-429X-16-2
36. Nordio G, Henningsson M, Chiribiri A, Villa ADM, Schneider T. 3D myocardial T₁ mapping using saturation recovery. *J Magn Reson Imaging.* 2017;46:218-227. doi:10.1002/jmri.25575
37. Marty B, Vignaud A, Greiser A, Robert B, De Sousa PL, Carlier PG. Bloch equations-based reconstruction of myocardium T₁ maps from modified look-locker inversion recovery sequence. *PLoS One.* 2015;10:e0126766. doi:10.1371/journal.pone.0126766
38. Lima da Cruz GJ, Velasco C, Lavin B, Jaubert O, Botnar RM, Prieto C. Myocardial T₁, T₂, T₂^{*}, and fat fraction quantification via low-rank motion-corrected cardiac MR fingerprinting. *Magn Reson Med.* 2022;87:2757-2774. doi:10.1002/mrm.29171
39. Christodoulou AG, Shaw JL, Nguyen C, et al. Magnetic resonance multitasking for motion-resolved quantitative cardiovascular imaging. *Nat Biomed Eng.* 2018;2:215-226. doi:10.1038/s41551-018-0217-y
40. Shaw JL, Yang Q, Zhou Z, et al. Free-breathing, non-ECG, continuous myocardial T₁ mapping with cardiovascular magnetic resonance multitasking. *Magn Reson Med.* 2019;81:2450-2463. doi:10.1002/mrm.27574
41. Hamilton JI, Jiang Y, Eck B, Griswold M, Seiberlich N. Cardiac cine magnetic resonance fingerprinting for combined ejection fraction, T₁ and T₂ quantification. *NMR Biomed.* 2020;33:1-17. doi:10.1002/nbm.4323
42. Wang X, Rosenzweig S, Roeloffs V, et al. Free-breathing myocardial T₁ mapping using inversion-recovery radial FLASH and motion-resolved model-based reconstruction. *Magn Reson Med.* 2023;89:1368-1384.
43. Hansen MS, Sørensen TS, Arai AE, Kellman P. Retrospective reconstruction of high temporal resolution cine images from real-time MRI using iterative motion correction. *Magn Reson Med.* 2012;68:741-750. doi:10.1002/mrm.23284

SUPPORTING INFORMATION

Additional supporting information may be found in the online version of the article at the publisher's website.

FIGURE S1. (A) Results of the numerical simulations for a heart rate of (A) 50 bpm, (B) 80 bpm and (C) 100 bpm, showing T₁ maps estimated without motion (Reference), without 30% of systolic time frames (2s MAP) and using the proposed motion-corrected MAP approach (2s mcirMAP) without 20% of systolic time frames. In addition, pixel-wise differences to the reference are shown.

FIGURE S2. Proposed motion-corrected MAP reconstruction (2s mcirMAP) for different numbers of iterations, ranging from 6 to 192 for two volunteers (A) and (B).

Blurring is visible for a low number of iterations (6). Higher numbers of iterations lead to an increase in noise. Here, 24 iterations were chosen, which led to robust reconstructions.

FIGURE S3. (A) Proposed motion-corrected MAP reconstruction (2 s mcirMAP) for different scales of motion field amplitudes. 100% corresponds to the estimated motion amplitude. 20% corresponds to a motion field that was scaled by 0.2, describing an underestimation of the cardiac motion. (B) Difference images show increasing errors with decreasing motion amplitudes.

FIGURE S4. Cardiac motion resolved images reconstructed for two different subjects (A and B) using the approach described in.¹⁰ For a total scan time of 8 s, this approach yields motion-resolved images with stable contrast. Reducing the scan time to 2.3 s leads to contrast variations between different cardiac phases and, in some cases, to a strongly reduced contrast between

blood and myocardium which does not allow for accurate cardiac motion estimation. For better visualization, the temporal profiles (indicated by the white line in Phase 3 and 2, respectively) are shown over three cardiac cycles. Each cardiac cycle is resolved with 12 images.

TABLE S1. T1 times in the phantom for the IR-SE reference, 16 s MAP and 2 s MAP for simulated heart rates of 50 bpm and 80 bpm. No significant differences were found between reference and 2 s MAP for both heart rates. Values are shown as mean \pm SD.

How to cite this article: Kerkering KM, Schulz-Menger J, Schaeffter T, Kolbitsch C. Motion-corrected model-based reconstruction for 2D myocardial T1 mapping. *Magn Reson Med.* 2023;90:1086-1100. doi: 10.1002/mrm.29699